

Corrosion of Copper in Deaerated and Oxygenated 0.1M H₂SO₄ Solutions under Controlled Conditions of Mass Transfer

Shatha A.Sameh*, Issam K.Salih*, Sadiq H.Alwash**
& AsawerAL-Waisty*

Received on:31/12/2007

Accepted on:31/12/2008

Abstract

The corrosion behavior of copper in deaerated and oxygenated 0.1 H₂SO₄ solutions has been investigated using the rotating cylinder electrode under turbulent flow conditions. Potentiostatic polarization measurements were carried out at different bulk temperatures of 283, 288, 293 and 298 K and various speeds of rotation viz 100, 200, 300 and 400 r.p.m. The anodic dissolution of copper and the hydrogen evolution reaction, in deaerated and oxygenated solutions, are activation controlled processes dependent on the temperature of the solution. The anodic dissolution of copper is not mass transfer controlled. The results are consistent with a mechanism which suggests that oxidation of copper takes place in two steps of one electron each. The second step, i.e., cuprous ion (Cu⁺) oxidation, is the rate controlling. Moreover, the mechanism of hydrogen evolution reaction is a proton discharge upon the metal surface. The charge transfer of the oxygen reduction reaction is a 2e process in the range of bulk temperatures employed, i.e., the oxygen reduction is controlled by 2e process. Furthermore, the limiting current density value of the oxygen reduction reaction increases as the velocity of the fluid increases. The results, at a constant bulk temperature are consistent with Eisenberg et al theory for mass transfer to a rotating cylinder electrode surface.

Keywords: Corrosion, Copper, H₂SO₄, rotating cylinder electrode.

تآكل النحاس في محاليل حامض الكبريتيك (0.1M) الخالية من الاوكسجين والمشبعه به عند ظروف انتقال الكتله المسيطر عليها

الخلاصة

تم دراسة السلوك التآكلي للنحاس في محلول حامض الكبريتيك ذو تركيز 0.1 مولاري خالٍ من الاوكسجين ومشبع به عند ظروف جريان مضطرب باستخدام منظومة قطب اسطواني دوار . أجريت تجارب الاستقطاب بالمجهاد الساكن في درجات حرارة مختلفة (283، 288، 293، 298 كلفن) وبسرعة تدوير مختلفة (100، 200، 300، 400 دورة / دقيقة). بينت النتائج ان كلا من حركية ذوبان الانود وتفاعل تحرر الهيدروجين في محاليل خالية من الاوكسجين ومشبعه به ، محكومة بطاقة التنشيط وتعتمد على درجة حرارة المحلول . ان حركية ذوبان الانود غير محكومة بانتقال الكتلة . وعليه فإن النتائج المتحققة متوافقة مع ميكانيكية حدوث اكسدة النحاس في مرحلتين (تحرير الكترولون واحد في كل مرحلة) ، وان ذوبان النحاس محكوم بالمرحلة الثانية التي تتضمن اكسدة ايون النحاس (Cu⁺) ، و ميكانيكية تفاعل تحرر الهيدروجين محكومة بمرحلة اختزال ايون الهيدروجين (H⁺) على سطح المعدن. اظهرت نتائج الدراسة ان اختزال الاوكسجين محكوم بعملية الكترولونين حيث ان شحنة تفاعل اختزال الاوكسجين هي الكترولونين في مدى درجات الحرارة المعتمده . كما وان قيمة كثافة التيار المحدد لتفاعل اختزال الاوكسجين تزداد بزيادة سرعة تدوير المحلول. وعليه فإن النتائج المستحصلة بثبات درجة حرارة المحلول متوافقة مع نظرية ايزنبرغ لأنتقال الكتلة الى سطح قطب اسطواني دوار

* Chemical Engineering Department, University of Technology/ Baghdad.

** Chemical Engineering Department, College of Engineering, University of Baghdad/ Baghdad.

Nomenclatures

A	Frequency Factor (constant)
ba	Anodic Tafel slope, V/decade
bc	Cathodic Tafel slope, V/decade
C _b	Concentration (bulk), mol/l
D	Diffusion coefficient, m ² /s
d	Cylinder diameter, mm
f	Faraday's constant, 96.5kJ/V.mol
ΔG*	Activation energy, kJ/mol
h	Cylinder height, mm
i _L	Limiting current density, mA/cm ²
n	Number of electrons transferred
R	Gas constant, 8.31 J/mol.K
r _i	Cylinder inside radius, mm
r _o	Cylinder outside radius, mm
T	Absolute temperature, K
V	velocity of fluid, m/s
Z	charge transfer
α	Transfer coefficient
ν	Kinematics viscosity, m ² /s
HER	Hydrogen evolution reaction
RCE	Rotating cylinder electrode
r.p.m	Rotation per minute
SCE	Standard calomel electrode

1. Introduction

There are several industrial operations which involve acid flow system in which an acid solution moves past a metal surface such as: steel strips pickling, industrial acid cleaning and oil well acidizing. Furthermore, acids are widely used in manufacturing processes of different industrial operations. In any case, flow is important.

Flow affects only those corrosion processes which are controlled by transfer of reactants to, and products from, the metal surface, i.e., mass transfer controlled process^{1, 2}. On mild steel and a large number of other metals and alloys, transfer of oxygen to the cathodic area is often rate controlling^{3, 4}. Whereas, with relatively noble metals such as copper the rate of diffusion of metal ions away from the surface may be the controlling factor⁵⁻⁷.

Transfer of oxygen to the metal surface is affected by a

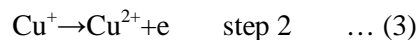
combination of convection and diffusion. The later predominates at the surface. The effect of flow is to increase the convection in the neighbourhood of metal surface, to decrease the thickness of the diffusion boundary layer⁷ and to supply the cathodic reactants, e.g. oxygen at a faster rate^{8,9}. In short, the reduction of oxygen becomes a more facile process.

The corrosion rates of a rotating iron cylinder and/or disk in deaerated acid solutions was reported by several workers¹⁰⁻¹⁴. They have shown that the corrosion rate was independent of the rotation rate. This body of results implies that iron dissolution and hydrogen evolution reactions are not mass transfer controlled under these circumstances. Similar results leading to the same conclusions on the anodic dissolution of nickel in deaerated sulfuric acid solutions have been obtained by Alwash^{4,15} and Turner et al¹⁶.

The dissolution reaction of copper in deaerated sulfuric acid solution can be represented¹⁷⁻²¹ as:



This reaction takes place in two steps of one electron each^{20,21}



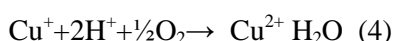
Where step 1 is in equilibrium condition and step 2 is the rate limiting condition. This may imply that step 2 is the slower step in the reaction sequence, i.e., the copper dissolution is an activation controlled process.

In oxygen saturated acid solutions, the corrosion rate of iron increases with increasing velocity of the solution^{10,13,22,23}. These results can be interpreted as indicating metallic corrosion under mass transfer control by the cathodic

reaction, i.e., the anodic reactions of iron are activation controlled processes.

A similar result leading to the same conclusions on the anodic dissolution of nickel in oxygenated 0.01N sulfuric acid solution under controlled condition of mass transfer has been obtained by Alwash⁴.

In aerated acid solutions, the rate determining step during the dissolution of copper is once again, the oxidation of cuprous ion (Cu⁺)^{18,24,25}:



This implies that the anodic dissolution of copper in aerated acid solutions is an activation controlled process.

However, it is well known that, in the presence of oxygen in acid solutions, two cathodic reactions take place which are hydrogen evolution reaction (HER) and oxygen reduction reaction^{26,27}. The first reaction, i.e., HER, is an activation controlled process^{4,23,26,27}. It was stated earlier, that oxygen transfer to the cathodic area is often rate controlling⁴, i.e., a mass transfer controlled process. Therefore, the effect of flow on the limiting current density (i_L) of the oxygen reduction reaction in acid solutions is to increase i_L as the flow increases.^{4,23,28-31}

In summary, the previous work reveals that the anodic dissolution of copper in deaerated and oxygen saturated acid solutions is an activation controlled process.

It is well known, in general, that the rate of corrosion of metals increase with increasing temperature, i.e., temperature affects corrosion reactions which are activation controlled process^{4,15,32-34}. It was stated earlier that the anodic dissolution of copper in deaerated and oxygen saturated acid solutions is an activation controlled process. Therefore, it would be expected that temperature will stimulate the corrosion reactions of copper in acid solutions.

The purpose of the present work is to investigate the corrosion rate of copper in deaerated and oxygenated 0.1M

H₂SO₄ solutions using the rotating cylinder electrode (RCE) system to provide quantified hydrodynamic mass transfer conditions and potentiostatic polarization technique for different values of velocity and temperature.

2. Experimental Work

The apparatus used in this work consisted of the following main parts, a supporting frame work, RCE assembly, polarization cell, constant temperature bath, a potentiostat and supplying unit of oxygen and nitrogen.

The RCE assembly shown in Fig. (1), consisted of:

1. A rotating cylinder and electrode shaft (the RCE)
2. A driving shaft, bearing unit and slip ring unit (the electrode mounting).
3. Motor and speed controller (the driving unit).

The design provided for a cylinder which was detachable from the electrode shaft, having the following dimensions:

$$r_0 = 15 \text{ mm}$$

$$r_1 = 8 \text{ mm}$$

$$h = 20 \text{ mm}$$

The specimens were cut and turned down to shape and size from 50 mm diameter rod of high purity copper having total purity of Cu =99.85%. The composition of copper being given in Table (1)³⁵. The analysis was done by the Central Organization for Standardization and Quality Control.

Before each test the electrode surface was prepared by grinding on successive grades of emery paper of 400,800 and 1000 grit respectively. Then the specimen was washed with distilled water, rinsed with acetone, dried with clean tissue paper and kept in a desiccator over silica gel before use³⁶.

The electrochemical tests were carried out in a polarization cell, which consists of a cylindrical glass vessel of a capacity of 2.5l. Bulk temperature control was achieved by using a constant temperature bath supplied with a refrigerating unit. Three electrode cells were used. The working electrode was in a cylindrical

form. Saturated calomel electrode (SCE) was used as a reference electrode with Lugging capillary tip placed at 1-2mm from the working electrode surface³⁷. Platinum counter electrode was used as an auxiliary electrode.

The test solution (0.1 M H₂SO₄) was prepared from analar grade concentrated sulfuric acid diluted with distilled water.

The experiments were carried out to determine the polarization curves (cathodic and anodic) of copper in deaerated and oxygenated 1000 ml 0.1M H₂SO₄ solutions. The experiments were made under isothermal conditions at four test solution bulk temperatures viz, 283, 288, 293 and 298K and under turbulent flow conditions at four controlled rotating speeds, i.e., 100, 200, 300 and 400 r.p.m. Each experiment involved electrochemical polarization of copper electrode, from -0.9V to +1.6V (SCE) with manual scan rate of 20×10^{-3} V/min, using a potentiostat (Wenking LT87). Each test was done twice, and if reproducibility was in doubt a third test was carried out. In addition each specimen was used one time only.

Prior to every experiment, nitrogen or oxygen was allowed to bubble into the solution at a rate of 300 ml /min for a period of 30 min to ensure complete deaeration or oxygen saturation of the solution. Thereafter, and at the start of electrochemical polarization, the gas rate was reduced to 25ml / min.

The detailed design of the apparatus and the experimental work were described elsewhere³⁸.

3. Experimental Results and Discussion

3.1) Deaerated solutions

The potentiostatic polarization curves for deaerated solutions are shown in Figs. 2 to 5.

The Cathodic Region

The cathodic curves in Figs. 2 to 5, show the presence of two linear regions and a limiting current between them. This can be explained according to the well acceptable fact that HER is the only possible reaction in deaerated acids. Kim and Nobe³⁹ reported that HER occurs at

two different regions, viz; hydrogen ion discharge which occurs at low cathodic over potentials (the upper region) and water discharge which occurs at higher cathodic over potentials (the lower region). The present result is in agreement with other workers,^(39, 40) who obtained similar cathodic polarization curves for corrosion of copper in deaerated acid solutions. From corrosion point of view; the upper region is of greater interest than the lower one. However, Stern⁴¹ suggested that the limiting current between the two linear regions is an indication of proton discharge process to be limited by mass transfer.

The cathodic Tafel slope, b_c , values of the upper linear region are in the range 110-127mV /decade. This is in agreement with values reported by Fontana and Greene²⁶ and Kim and Nobe³⁹.

The transfer coefficient α , for the upper linear cathodic region is found to be 0.47 – 0.51, by applying the following equation⁴²:

$$b_c = 2.303 RT / \alpha nF \quad \dots(5)$$

This result indicates that the mechanism of HER is discharge rate determined followed by electroodic desorption^{42, 43}.

Table (2) shows the values of the cathodic current density, at a given cathodic potential (-300 mV), at different temperatures and speeds of rotation. The table shows that the cathodic current density is temperature dependent only.

In summary, in this region, the controlling step of HER is the discharge of the proton upon the metal surface which is an activation controlled process. This result is in agreement with previous works^{3, 15, 23, 32-34}, i.e., temperature affects corrosion reactions which are activation controlled processes.

The Anodic Region

The anodic polarization curves in Figs. 6 to 9 show the presence of two linear regions. The anodic Tafel slope, b_a , values of the higher and lower anodic over potential regions are 130 and 30-40

mV/decade respectively. These results are in reasonable agreement with those reported by other workers^{20,21} for corrosion of copper in deaerated sulfuric acid solutions. They revealed that the oxidation of copper takes place in two steps of one electron each, as represented by equations 2 and 3, and step 2 is the rate limiting condition.

The anodic current density values taken at +80mv, at different bulk temperatures and various speeds of rotation, are given Table (3). The table shows that the anodic current density is temperature dependent only. This indicates that anodic dissolution of copper in deaerated sulfuric acid solution is under activation control. The result is in agreement with previous works^{3,15,23,32-34}, i.e., temperature affects corrosion reaction which are activation controlled processes.

In summary, the copper anodic dissolution in deaerated acid solutions is under activation control, i.e., it is not affected by flow variation and increases as temperature increases. The results are in agreement with a suggested mechanism for copper dissolution that takes place in two steps, and comprise a rate determining step.

The corrosion current density values, calculated according to the 4-point method,^{44, 45} at different bulk temperatures and various speeds of rotation are given in Table (4). The table shows that the corrosion current density is temperature dependent only.

The rate of the reaction may be expressed by the Arrhenius equation³², viz :

$$\text{rate of reaction} = Ae^{-\Delta G^*/RT} \dots(6)$$

and a plot of log rate of reaction versus 1/T should produce a straight line having a slope = $-\Delta G^*/2.303 R$.

The corrosion rates in Table (4) were plotted versus the reciprocal of temperatures (the plot is shown elsewhere³⁸). The data fall around a straight line which was drawn as a good

fit and has a slope = -2.8, and, $\Delta G^*=53.8$ KJ/mol (12.86 Kcal/mol).

This result is in a good agreement with a reported value for activation energy of about 12.0 Kcal/mol for corrosion of copper in 1 N sulfuric acid solution⁴⁶.

Moreover, the corrosion rate values in Table (4) are independent of rotation rates. This result is consistent with similar reported works, but, on iron¹⁰⁻¹⁴ and on nickel^{4, 15, 16}. This implies that copper dissolution and HER in deaerated sulfuric acid solutions are not mass transfer controlled.

3.2) Oxygenated Solutions

The potentiostatic polarization curves for oxygenated solutions are shown in Figs. 10 to 13.

The Cathodic Region

The cathodic curves, in Figs. 10 to 13, show the presence of a linear region and, also, a limiting current density at high over potential.

The cathodic Tafel slope values of the linear region are in the range 175-190 mV/decade, and they are nearly constant with increasing velocity. These values are higher than the corresponding values in deaerated solutions. This can be attributed to the presence of another cathodic reaction, i.e., oxygen reduction reaction^{26, 27}.

Table (5) shows the values of the cathodic current density, at a given cathodic potential (-300mV) at different bulk temperatures and various speeds of rotation. The table shows that the cathodic current density is temperature dependent only. Moreover, the cathodic current density values are much higher than the corresponding values in deaerated solutions (see Table 2). This can be, once again, attributed to the presence of another cathodic reaction i.e., oxygen reduction reaction^{26, 27}.

At high overpotential, a limiting current density of the oxygen reduction reaction (i_L) appeared (see Figs.10 to 13). The values of i_L at different bulk temperatures and various speeds of rotation are given in Table (6). The table shows that i_L increases as the speed of rotation increases. The results are in

agreement with previous workers^{4, 23, 28-31}. The results in Table (6) are most readily discussed by reference to Figs. 14 to 17. These figures show that i_L is related to $v^{0.7}$ at a particular test solution bulk temperature, Figs 14 to 17 show, at each bulk temperature, there is almost a linear relationship between i_L and $v^{0.7}$ which when extrapolated passes through the origin. Therefore, the experimental data shown in Figs. 14 to 17 are in qualitative agreement with Eisenberg et. al⁴⁷ theory for mass transfer to a rotating cylinder electrode and represented by the expression:

$$i_L = 0.079ZFC_b v^{0.7} d^{-0.3} v^{-0.344} D^{0.644} \dots (7)$$

The increase in i_L with v is explained as follows; it was noted before that the effect of increasing velocity is to decrease the thickness of the diffusion boundary layer⁷ and to supply oxygen at a faster rate^{8,9} i.e., the reduction of oxygen becomes a more facile process.

It is well established, that oxygen reduction reaction is found to proceed by a 2 or 4 electron process^{4, 23, 31}, i.e., z in the Eisenberg et al equation⁴⁷ is 2 or 4. Therefore, the theoretical values of the limiting current density for both the 2 electron (2e) and 4 electron (4e) processes in test solution are also shown in Figs. 14 to 17 (solid lines)*. The experimental data fall around the 2e line indicating that the charge transfer of the oxygen reduction is controlled by a 2e process i.e., the oxygen reduction is controlled by a 2e process.

*The theoretical values of i_L of the oxygen reduction reaction at any value of r.p.m can be calculated from the kinematic viscosity⁴⁸, the diffusion coefficient⁴ and concentration of oxygen⁴⁹, using Eq. (7) see Table (7).

Table (6) also shows that i_L is slightly increased with an increase in bulk temperature. This may be attributed to an increase in the oxygen diffusion coefficient (D) and a lowering of the kinematics viscosity (v)^{4,31} of the

solution as the temperature increases (see Eq.7.)

The Anodic Region

The anodic polarization curves in Figs. 10 to 13 show a linear region. The anodic Tafel slope values are in the range 30-40 mV / decade, which is the same range obtained above for the corresponding values in deaerated solution. Moreover, the present result is in a reasonable agreement with that obtained by da Costa and Agostinh²¹ who reported a value of 42mV / decade in oxygenated (and deaerated) sulfuric acid solutions. Therefore, the presence of oxygen has no specific influence on the mechanism of anodic dissolution.

The anodic current density values at 80mv, at different bulk temperatures and various speeds of rotation, are given in Table (8). The table shows that the anodic current density is temperature dependent only. This indicates that anodic dissolution of copper in oxygenated sulfuric acid solution is under activation control. The result is in agreement with previous works^{3, 15, 23, 32-34}, i.e., temperature affects corrosion reactions which are activation controlled processes. Moreover, Table (8), also shows that the current density values are not affected by speed of rotation. Therefore, the anodic dissolution of copper is not mass transfer controlled. The results are in agreement with a suggested mechanism that: in aerated acid solutions, the rate determination step during the dissolution of copper is the oxidation of cuprous ion (Cu⁺)^{18, 24, 25}, (see Eq.4).

The corrosion current density values, calculated according to Tafel extrapolation technique⁵⁰, at different bulk temperatures and various speeds of rotation are given in Table (9). The table shows that the corrosion current density is temperature dependent only, which is in agreement with results of Zembura^{19,51} who reported that the corrosion rate of copper in aerated sulfuric acid solution becomes activation controlled at 298 K. The present work was confined to temperature range 283-298K.

The activation energy value was calculated in a similar manner to that in deaerated solution i.e., from Arrhenius plot, and found equals to 44KJ / mol (10.5kcal/mol). This value is lower than that obtained in deaerated solution, i.e., the energy required for corrosion reaction is decreased in oxygenated solution. This means a greater tendency for copper to corrode in oxygenated solution. This can be attributed to the presence of another cathodic reaction, i.e, oxygen reduction reaction in addition to HER^{26,27}.

4. Conclusions

The anodic dissolution of copper and HER, in deaerated and oxygenated 0.1 M sulfuric acid, are activation controlled processes, dependent on the temperature of the solution. The anodic dissolution of copper is not mass transfer controlled. The results are consistent with a mechanism which suggests that oxidation of copper takes place in two steps of one electron each. The second step, i.e., cuprous ion (Cu⁺) oxidation, is the rate controlling.

The mechanism of HER is a proton discharge upon the metal surface. The charge transfer of the oxygen reduction reaction is 2e process, i.e., the oxygen reduction is controlled by 2e process. Furthermore, the i_L value of the oxygen reduction reaction increases as the velocity of the fluid increases. The results, at a constant bulk temperature, are consistent with Eisenberg et al⁴⁷ theory for mass transfer to a RCE.

References

- [1]. Shreir L.L., Jarman R.A. and Burstein G.T., Corrosion (2nd edition) Butterworth – Heinemann, Oxford, Boston, (1994).
- [2]. Pierre R. Roberge, "Hand Book For Corrosion Engineering"(1st edition) McGraw Hill N.Y. (2000).
- [3]. Stansbury E.E. and R.A. Buchanan, " Fundamentals of electrochemical Corrosion" ASM International (2000).
- [4]. Alwash, S.H., Ph.D. Thesis, UIMIST (1977).
- [5]. Laque, F.L., Corrosion, 13,303t (1957).
- [6]. Copson, H.R., Corrosion, 16,86t (1960).
- [7]. Ross, T.K. and Hitchen, B.P.L., Corros. Sci, 1,65 (1961).
- [8]. Hatch, G.B. and Rice, O., Ind. Eng. Chem, 37,752 (1945).
- [9]. Mahato, B.K., Voora, S.K. and Shemitt, L.W., Corros. Sci, 8,173 (1968).
- [10]. Makrides, A.C, Komodromos, N.M. and Hackerman, N., J. electrochem Soc., 102,363 (1955).
- [11]. Makrides, A.C., J. electrochem Soc., 107,869 (1960).
- [12]. Foroulis, Z.A. and Uhlig, H.H., J. electrochem Soc, 111, 13 (1964).
- [13]. Ross, T.K., Wood, G.C. and Mahmud, I., J. electrochem Soc, 113,334 (1966).
- [14]. Tobias, R.F. and Nobe, K., J. electrochem Soc, 122 (1), 65 (1975).
- [15]. Alwash, S.H., BSE / NACE, Middle East Corrosion Conf., Bahrain, 742 (1979).
- [16]. Turner, M, Thompson, G.E. and Brook, P.A., Corros. Sci, 13,985 (1973).
- [17]. Bumbulish, J. And Graydon, W.F., J. Electrochem. Soc., 109, 12 (1962).
- [18]. Ghandehari, M.H., Anderson, T.N. and Eyring, H., Corros. Sci, 16,123 (1976).
- [19]. Zembura, Z and Bugajski, Corros. Sci., 21,1 (1981).
- [20]. Mattison, E. And Bockris, J.O' M, Trans. Faraday Soc., 55, 1586 (1959).
- [21]. da Costa, S.L.F.A and Agostinho, Corrosion, 45,6 (1989).
- [22]. Friend, J.N., and Dennett, J.H., J Chem. Soc., 121,41 (1922).
- [23]. Jaralla, A.A., Ph.D. Thesis, UIMIST (1984).
- [24]. Lu, B.C.Y. and Graydon,

- W.F., Can.J. Chem., 32, 153 (1954).
- [25]. Mayanna, S.M. and Setty, T.H.Y., Corros.Sci., 15,627 (1975).
- [26]. Fontana, M.J. and Greene, N.D., Corrosion Eng., 2nd ed. McGraw-Hill, N.Y. (1978).
- [27]. Uhlig, H.H. and Revie, R.W., Corrosion and Corrosion Control, 3rd.ed. John Wiley, N.Y. (1985).
- [28]. Damjanovic, A., Genshaw, M.A. and Bockris, J.O' M, J electrochem. Soc., 114, 466 (1967).
- [29]. Postlethwaite, J. and Sephton, J., Corros. Sci. 10, 775 (1970).
- [30]. Levich, V.G. Physicochemical Hydrodynamics, Prentice Hall, Inc., Englewood Cliffs, N.J. (1962).
- [31]. Alwash, S.H., Ashworth, V, Shirkhazadeh, M. and Thompson, G.E., Corros. Sci., 27, 1301 (1987)
- [32]. Hackerman, N., Ind. Eng. Chem., 44, 1752 (1952).
- [33]. Gregory, D.P. and Riddiford, A.C., J. electrochem. Soc., 107, 12 (1960).
- [34]. Popic, J.P. and Drazic, D.M., Bulletin of the Chemists and Technologists of Macedonia Chem.Soc., 23(2), 93 (2004).
- [35]. Central Organization for Standardization and Quality Control Jadiryah, Baghdad.
- [36]. Annual Book of ASTM standards, Part 10, G31 (1980).
- [37]. Annual Book of ASTM Standards, Part 10, G59 (1980).
- [38]. Al-Wasity, A.A.R., M.Sc. Thesis, University of Technology (1999).
- [39]. Kim, C.P. and Nobe, K., Corrosion, 27, 9 (1971).
- [40]. Tohala, N., Ph.D. Thesis, UMIST (1976)
- [41]. Stern, M., J. electrochem. Soc., 103, 609 (1955).
- [42]. Bockris, J.O' M. and Potter, E.C., J. electrochem. Soc., 99, 169 (1952).
- [43]. Bockris, J.O' M. and Reddy, A.K.N., Modern Electrochemistry, Vol 2, Plenum Press, N.Y. (1970)
- [44]. Jankowshi, J. and Juchnifwicz, R. Corros. Sci. 20, 841 (1980).
- [45]. Laranz, W.J., Karlsruhe, F.R.G. and Mansfeld, F., Proc. 8th Intn. Congr. on Metallic Corrosion, Germany, Sept. (1981).
- [46]. Haruyama, S. and Kaneko, M., Corros. Sci., 15, 35 (1975).
- [47]. Eisenberg, M., Tobias, C.W. and Wilke, C.R., J. electrochem. Soc., 101, 306 (1954).
- [48]. Grober, H., Erk, S. and Grigull, U., Fundamentals of Heat Transfer, p.497, McGraw - Hill, N.Y. (1961).
- [49]. Perry, R.H. and Chilton, C.H. Chem. Engrs. Hand book, 5th ed., McGraw - Hill, N.Y. (1973).
- [50]. Stern, M. and Geary, A.L., J. Electrochem. Soc., 104, 56 (1957).
- [51]. Zembura, Z., Corros. Sci., 8, 703 (1968).

Table (1): Composition of Copper (wt %)

Sn	Zn	P	Fe	Si	Mn	As	Sb	Al	S	Cu
0.0485	0.02	0.036	0.003	0.003	0.01	0.005	0.004	0.007	0.009	remainder

Table (2): The cathodic current density for deaerated solutions at (-300mv), $\mu\text{A} / \text{cm}^2$

Temp. K	rpm			
	100	200	300	400
283	13	13	13	13
288	22	23	22	23
293	35	35	35	36
298	47	46	47	47

Table (3): The anodic current density for deaerated solutions at (+80 mv), $\mu\text{A}/\text{cm}^2$

Temp. K	rpm			
	100	200	300	400
283	1.19	1.20	1.20	1.20
288	2.41	2.40	2.40	2.41
293	2.65	2.50	2.63	2.54
298	3.50	3.50	3.60	3.50

Table (4): The corrosion rate for deaerated solutions , $\mu\text{A}/\text{cm}^2$

Temp. K	rpm			
	100	200	300	400
283	0.96	0.96	0.96	0.96
288	1.30	1.30	1.37	1.37
293	1.85	1.81	1.87	1.90
298	2.10	2.10	2.20	2.20

Table (5): The cathodic current density for oxygenated solutions at (-300 mv), $\mu\text{A} / \text{cm}^2$

Temp. K	rpm			
	100	200	300	400
283	0.10	0.10	0.10	0.10
288	0.18	0.20	0.20	0.19
293	0.20	0.29	0.30	0.31
298	0.33	0.34	0.34	0.35

Table (6): The limiting current density for oxygenated solutions, mA/cm^2

Temp. K	rpm			
	100	200	300	400
283	0.80	1.10	1.51	1.70
288	0.91	1.30	1.70	2.04
293	1.06	1.41	1.98	2.30
298	1.10	1.50	2.02	2.40

Table (7): Theoretical values of the limiting current density of the oxygen reduction reaction (2e and 4e), mA/ cm²

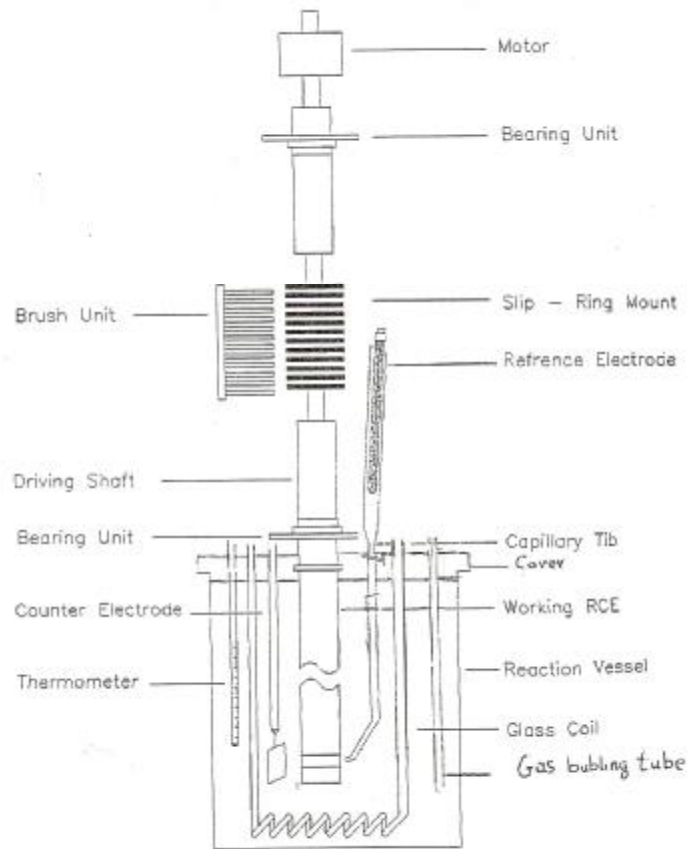
rpm	V ^{0.7} m/s	Bulk Temperature K°							
		283		288		293		298	
100	0.274	0.67	1.34	0.77	1.54	0.85	1.70	0.92	1.84
200	0.445	1.09	2.18	1.26	2.52	1.40	2.80	1.52	3.04
300	0.591	1.45	2.90	1.67	3.34	1.86	3.72	2.01	4.02
400	0.723	1.77	3.54	2.05	4.08	2.06	4.12	2.46	4.92

Table (8): The anodic current density for oxygenated solutions at (+800 mv/, μA/ cm²

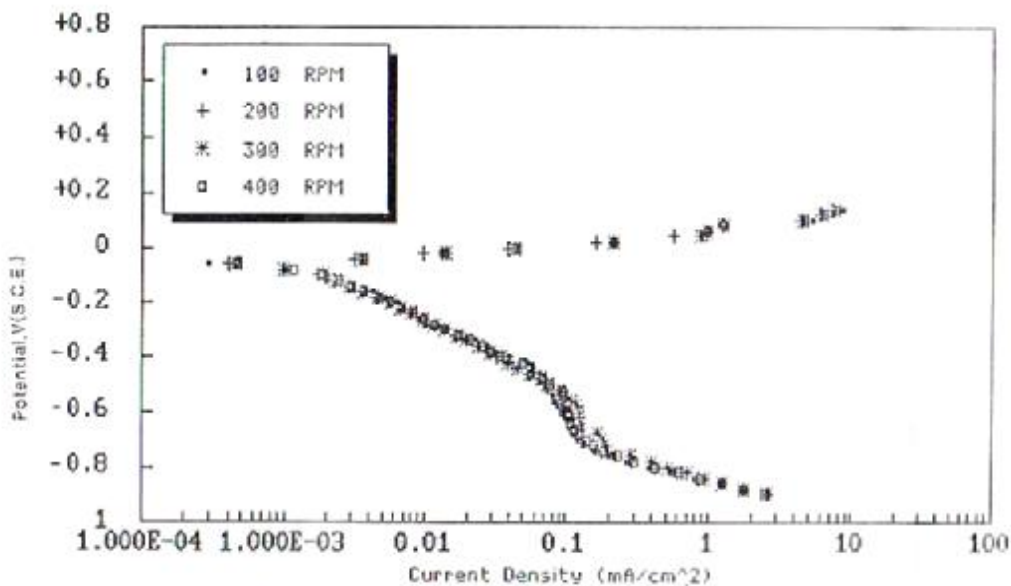
Temp. K	rpm			
	100	200	300	400
283	1.64	1.60	1.60	1.60
288	2.90	3.00	3.08	2.94
293	3.70	3.71	3.72	3.78
298	4.20	4.10	4.30	4.10

Table (9): The corrosion rate for oxygenated solution, μA / cm²

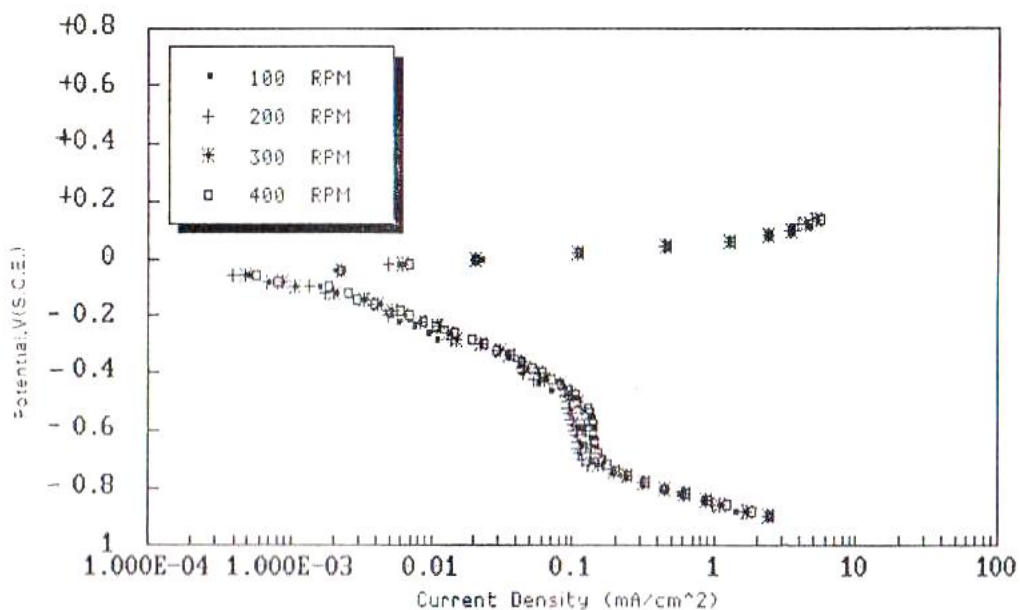
Temp. K	rpm			
	100	200	300	400
283	7.0	7.1	7.0	7.2
288	9.4	9.5	9.4	9.4
293	12.2	12.0	12.1	12.0
298	20.0	19.0	20.0	20.0



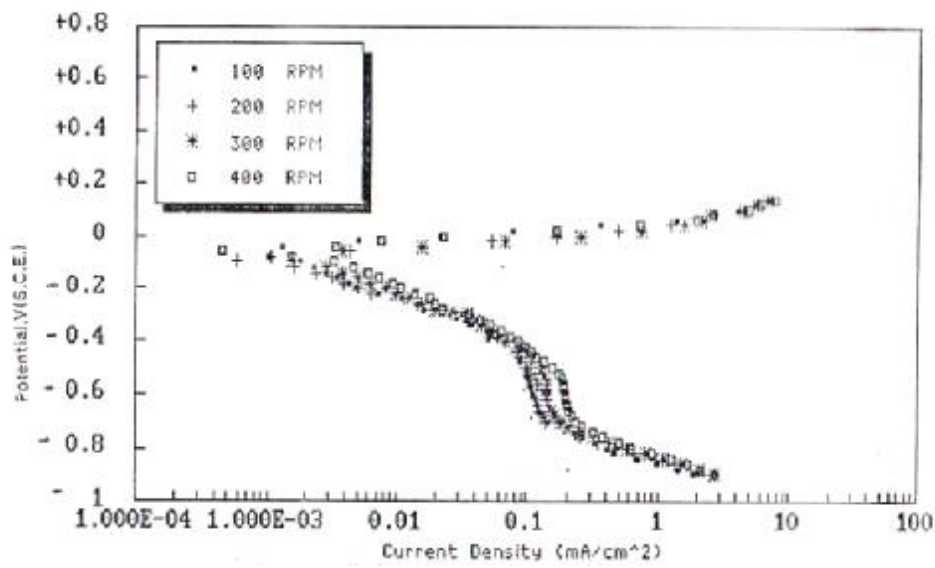
Figure(1): The rotating cylinder electrode assembly



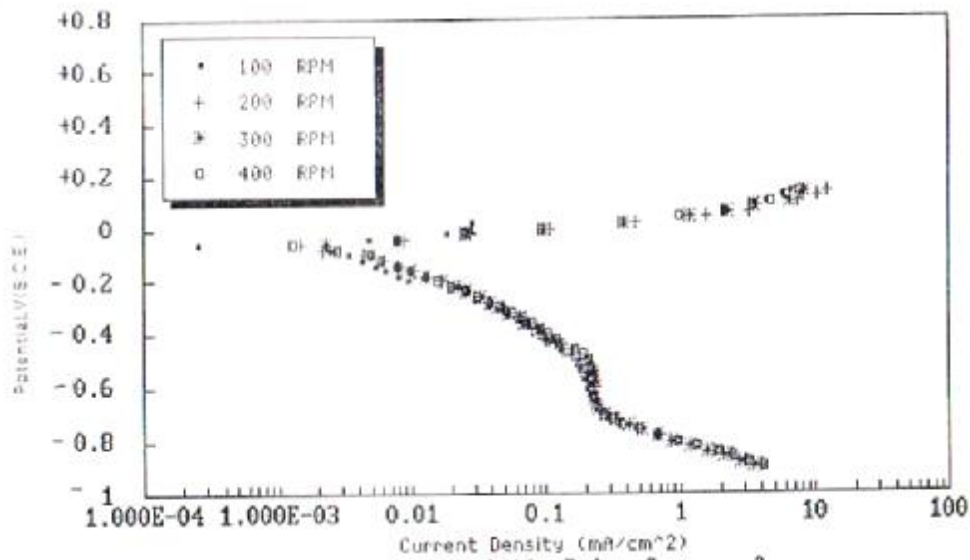
Figure(2): Potentiostatic polar curves of deaerated solution, temp.283K



Figure(3): Potentiostatic polar curves of deaerated solution, temp.288K



Figure(4): Potentiostatic polar curves of deaerated solution, temp.293K



Figure(5): Potentiostatic polar curves of deaerated solution, temp.298K

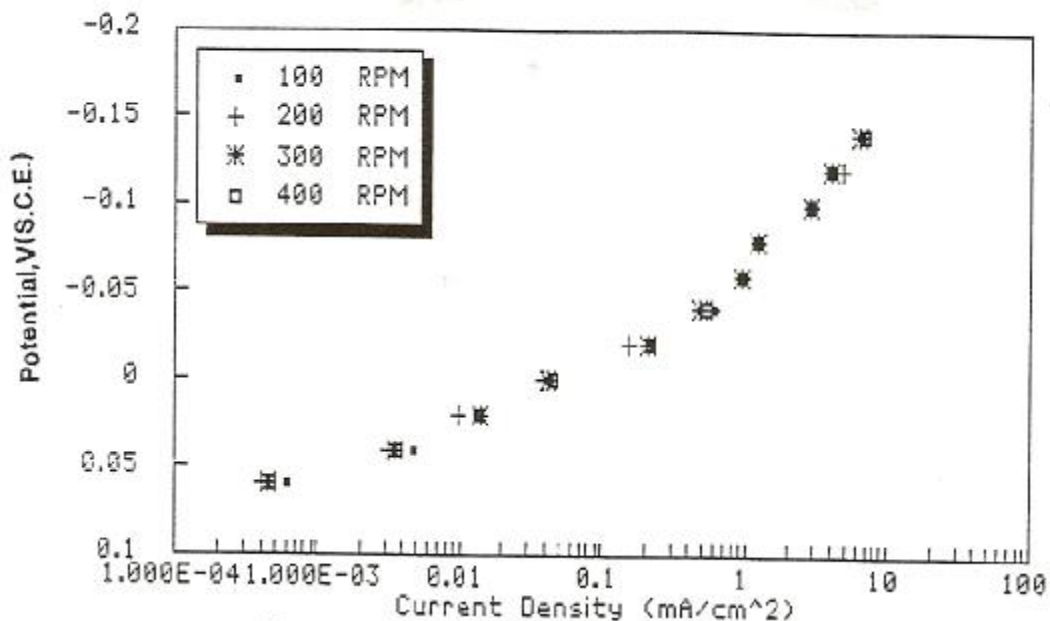


Figure (6): Anodic polarization curves of deaerated solution, temp. 283

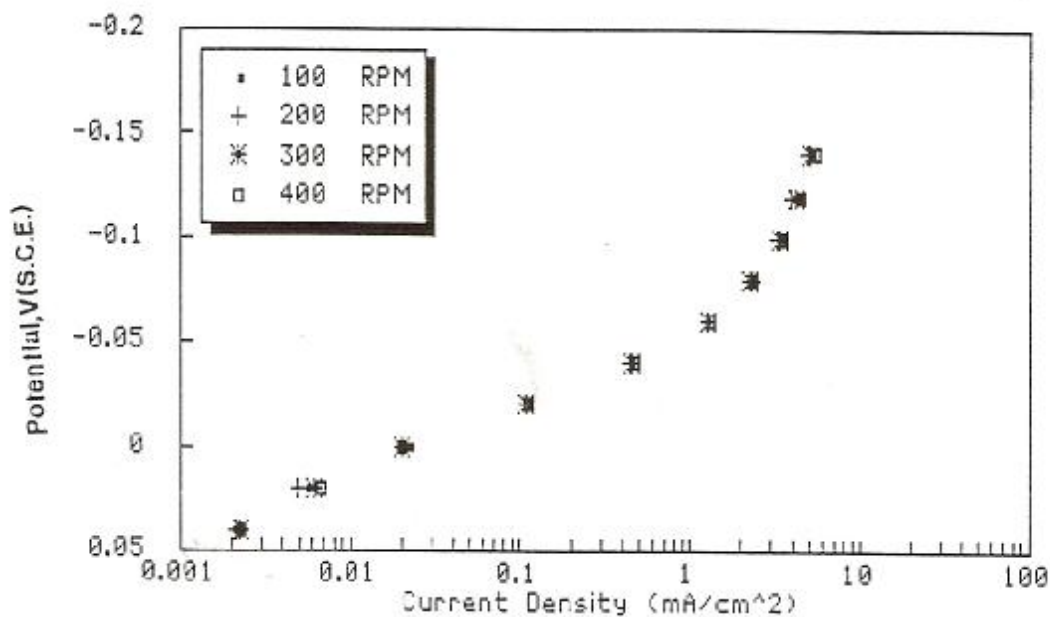


Figure (7): Anodic polarization curves of deaerated solution, temp. 288

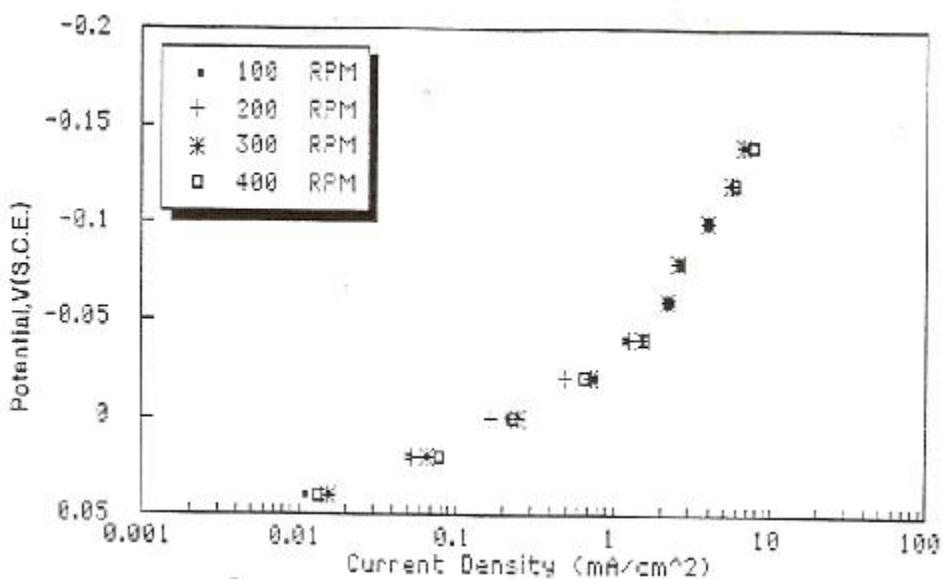


Figure (8): Anodic polarization curves of deaerated solution, temp. 293

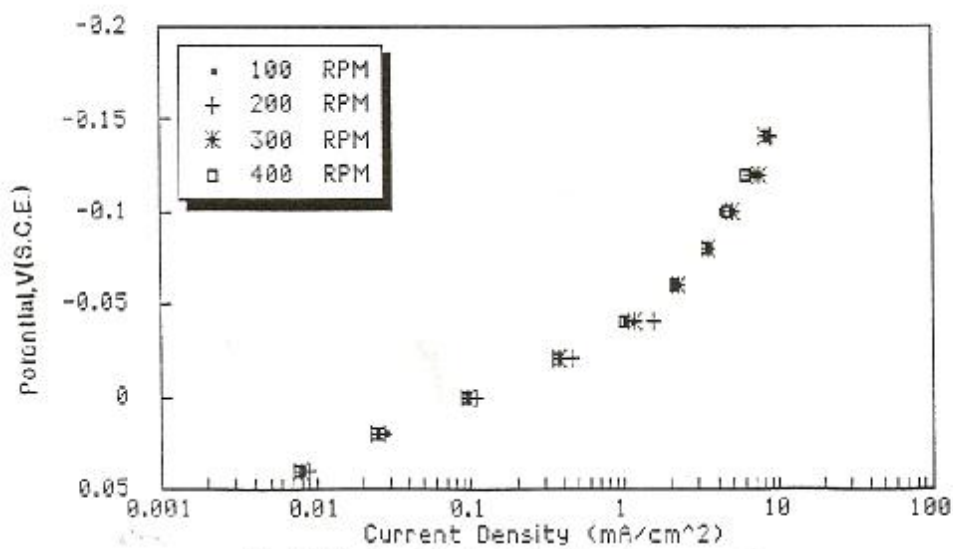


Figure (9): Anodic polarization curves of deaerated solution, temp. 298